

# **Stabilisation of Fe based nano-structures developed through mechanical milling**

A THESIS SUBMITTED IN PARTIAL FULFILLMENT OF THE  
REQUIREMENTS FOR THE DEGREE OF

**Bachelor of Technology**

**In**

**Metallurgical & Materials Engineering**

**By**

**SWASTIK MOHAPATRA (109MM0480)**

**SUMEET SEKHAR PATEL (109MM0451)**



**Department of Metallurgical & Materials Engineering**

**National Institute of Technology, Rourkela**

**2013**

# **Stabilisation of Fe based nano-structures developed through mechanical milling**

A THESIS SUBMITTED IN PARTIAL FULFILLMENT OF THE  
REQUIREMENTS FOR THE DEGREE OF

**Bachelor of Technology**

**In**

**Metallurgical & Materials Engineering**

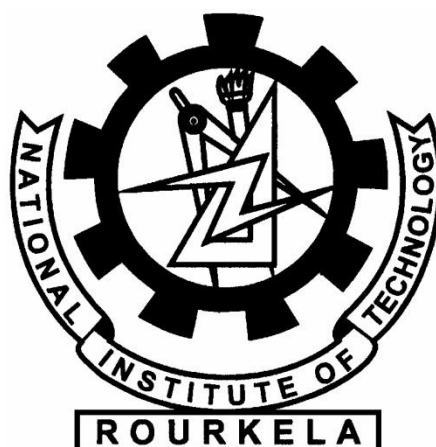
**By**

**SWASTIK MOHAPATRA (109MM0480)**

**SUMEET SEKHAR PATEL (109MM0451)**

**Under the guidance of:**

**Prof. S.C Mishra**



**Department of Metallurgical & Materials Engineering**

**National Institute of Technology, Rourkela**

**2013**

# ACKNOWLEDGEMENT

We record our sincere gratitude to **Prof. S.C. Mishra** and **Prof Suhrit Mula**, Dept. of Metallurgical and Materials Engineering for assigning us the project titled “Stabilization of Fe based nanostructures developed through mechanical milling”. Their encouragement and continuous guidance made it possible for us to comprehend the project better & successfully complete it. Their constant voice of advice and constructive criticism has been our source of inspiration.

We would also like to convey our heartfelt gratitude to **Prof Swadesh Kumar Pratihara**, Dept. of Ceramic Engineering for helping us with our project and guiding us while using the equipments under his supervision.

We are also thankful to our HOD **Prof. B. C. Ray** for supporting us with our project.

We are also thankful to **Mr. Uday Kumar Sahu, Mr. Rajesh Patnaik and Mr. S. Hembram** of Metallurgical and Materials Engineering Dept. for helping us throughout our project work.

Sumeet Sekhar Patel

109MM0451

Swastik Mohapatra

109MM0480

Bachelor of Technology

Metallurgical and Materials Engg.



**National Institute of Technology**

**Rourkela**

## **CERTIFICATE**

This is to certify that the thesis entitled, “**Stabilization of Fe based nanostructures developed by mechanical milling**” being submitted by **Sumeet Sekhar Patel (109MM0451)** and **Swastik Mohapatra (109MM0480)** in partial fulfilment of the requirements for the award of Bachelor of Technology Degree in **Metallurgical and Materials Engineering** at the National Institute of Technology, Rourkela (Deemed University) is an authentic work carried out by him under my supervision and guidance.

To the best of my knowledge, the matter embodied in the thesis has not been submitted to any other University / Institute for the award of any Degree or Diploma.

Date :

**Dr. S.C. Mishra, Professor**

Dept. of Metallurgical and Materials Engg.

National Institute of Technology, Rourkela-769008

# Contents

<b>S.no</b>		<b>Page no.</b>
<b>1.</b>	<b>Introduction.....</b>	<b>5</b>
1.1	Aim and objectives.....	6
<b>2.</b>	<b>Literature Review.....</b>	<b>7</b>
2.1	Preamble.....	7
2.2	Synthesis techniques of Nano-structured materials.....	8
2.3	Mechanical Alloying to prepare Iron based Nano-crystalline.....	15
2.4	Grain growth of Iron based Nano-crystalline prepared by Mechanical alloying .....	16
2.5	Grain growth stabilization.....	19
<b>3.</b>	<b>Experimental.....</b>	<b>25</b>
<b>4.</b>	<b>Result and Discussions.....</b>	<b>28</b>
4.1	Vickers' micro-hardness test results.....	28
4.2	Structural Characterization of Milled Samples.....	29
<b>5.</b>	<b>Conclusions.....</b>	<b>36</b>
<b>6.</b>	<b>Scope for further work.....</b>	<b>38</b>
<b>7.</b>	<b>References.....</b>	<b>39</b>

## **Abstract**

Synthesis of Fe based nanostructures developed by high energy ball milling has been carried out in the present study. Mixtures of Iron and Yttrium in the desired quantities were ball milled in stainless steel grinding media to prepare the required nanostructures. The powdered mixtures of 3 different compositions obtained were then pelletized in a pellet pressure machine. All the alloys were annealed at different temperatures up to 1200°C under high purity argon atmosphere. XRD analysis and micro hardness measurement were carried out for all the specimens to analyze their stability after annealing and to investigate the grain size stabilization caused by adding minute amounts of Yttrium. Lattice strain and crystallite size values calculated by using Scherer formula were analysed. Stable crystallite size (less than 100 nm) and constant micro hardness of the annealed samples can dictate its usefulness for high strength and other functional applications.

**Keywords:** Mechanical alloying; Nanostructures; Grain size stabilization; Micro hardness;

## 1. Introduction

Owing to its high strength, high range of properties and alloy forming capability, iron has a wide range of applications like structural applications, automobile, making of magnets, other house hold applications etc. Due to its high strength, low cost and availability it is a very commonly used metal. The properties of iron can be enhanced by adding alloying elements, performing heat treatment operations so as to induce the desired properties for a desired operation. In the nano scale, iron nano particles have found their usage in magnetic recording media and transformer cores. However, in nano scale, a very high surface area/volume ratio, a high value of surface energy and grain coarsening as a result sintering of nano particles at high temperature are a cause of concern. This can be improved by making nano structured iron and by solid solution of Iron and other materials like Nickel, Chromium etc. The grain growth while annealing at high temperature can be stabilized by zirconium, yttrium, tantalum etc. [1-3] K.A. Darling et al. found that zirconium is a strong stabilizer and tantalum is a moderate stabilizer of grain of nano crystalline Iron [3].

In this present study, nano-crystalline “Fe” and solid solution of “Fe-Y” are prepared by mechanical alloying (MA) in a Spex shaker mill. Fe-0.25 atom % Y and Fe-0.5 atom % Y formed complete solid solution after MA for 1500 min.

In the Fe-based powder, with increasing milling time the grain size of the MA powder decreases; however, the decrease in particle size is not linear with milling time. Milling time of 144 h. and more leads to serious cold-welding. The relative density of the as-sintered alloys is influenced by the particle size of the powders before sintering. The coarse particles lead to a low density in the sintered alloys. In the elongated particles the micro hardness is higher than that in the equiaxed grains, the main causes are higher density of the precipitated phase and the larger residual strain [4]. Mechanical milling increases hardness up to by the mechanism of grain refinement strengthening. Annealing reduces hardness and induces grain growth. The Vickers hardness of nanocrystalline grains shows less interaction towards Hall–Petch equation rather than coarse-grained powders annealed at high temperatures [5].

In the present study, Fe nanostructures were developed by mechanical alloying in a high energy shaker mill and yttrium is used to stabilize the nanograins. XRD analysis,

annealing under inert atmosphere, and microhardness measurement were used to investigate the stabilization effect of yttrium. Stable crystallite size (less than 100 nm) and constant microhardness of the annealed samples can dictate its usefulness for high strength and other functional applications.

### **1.1 Aims and objectives :**

The present work aims at :

- MA of three Fe-rich compositions, namely (1) Pure Fe, (2) Fe-Y<sub>0.25</sub> (3) Fe-Y<sub>0.5</sub>,
- Annealing of the above compositions at 500 °C, 700 °C, 900 °C, and 1200 °C.
- XRD analysis of all the above as-milled and annealed samples.
- Characterization of the crystal size and lattice strain of the above prepared samples by XRD.
- Study of effect of yttrium content on crystal size, lattice strain and micro hardness.
- Evaluation of mechanical properties and analysis of the annealed compacts: This would be done by evaluating mechanical properties, namely, microhardness.
- Study of effect of yttrium content on micro hardness.
- Study of effect of annealing temperature over crystal size and microhardness.
- Characterization of microstructural features of the selected annealed compacts by XRD to dictate its usefulness for high strength and other functional applications.



## 2. Literature review

### 2.1 Preamble

Iron is a most useful metal due to its high strength, high flexural rigidity, low cost and availability. It has a wide range of applications like structural applications, automobile, making of magnets, other house hold applications etc. So the properties of iron need to be enhanced for increasing its utilization and broadening its field of application. Use of Fe in nano technology has progressed well particularly in the magnetic recording media. But nano structures Fe faces the problem of sintering and grain coarsening when operated at high temperatures. This can be improved by making nano structured iron and by solid solution of Iron and other materials like Nickel, Chromium etc. The grain growth while annealing at high temperature can be stabilized by zirconium, yttrium, tantalum etc. [1-3] K.A. Darling et al. found that zirconium is a strong stabilizer and tantalum is a moderate stabilizer of grain of nano crystalline Iron [3].

High energy ball milling helps to produce nanostructured material, which allows powdered samples with different structures and novel properties to be obtained. Due to their small grain size, these materials are characterized by a rather high number of atoms located in the grain boundary. Also, they are very interesting from the magnetic point of view because the grain size approaches that of a magnetic domain, hence offering the possibility to eliminate the influence of the domain walls. It is well established that the intermetallic compounds prepared by mechanical alloying (MA) have a high structural disorder and are unstable.

Cui et al. [6] have studied structure and mechanical properties of high-nitrogen nickel-free austenitic stainless steels with a relative density of 99% fabricated by powder injection molding, conventional sintering, and solidnitriding [6].

D. Cai et al. studied Fe–Ni–Cr alloy system, optimum mechanical properties can be obtained by solution-treated at 1000 °C followed by conventional aging. When the solution temperature is above 1050 °C, the flake-like M3B2 precipitates appear along grain boundary and its formation impairs the strength and ductility.

## **2.2 Synthesis techniques of nanostructured materials**

Various techniques used to synthesize nanostructured materials include

1. Inert gas condensation,
2. rapid solidification processing,
3. electrodeposition,
4. sputtering,
5. crystallization of amorphous phases,
6. chemical processing and
7. Mechanical attrition (ball milling/ mechanical alloying).

Mechanical alloying (MA) is a technique that is used to produce homogeneous nano powders by blending elemental powder mixtures. It involves repeated welding, fracturing, and rewelding of powder particles in a high-energy ball mill. The non-equilibrium phases synthesized include supersaturated solid solutions, metastable crystalline and quasicrystalline phases, nanostructures, and amorphous alloys.

### **2.2.1 Importance of Mechanical milling**

Mechanical alloying (MA) is a solid-state powder processing technique that involves repeated cold welding, fracturing, and rewelding of powder particles in a high-energy ball mill. Earlier, the method of MA was developed in the 1970's for the production of thorium dispersed nickel (TD Nickel) based superalloys. MA has now the capability of synthesizing a variety of metastable phases starting from elemental powder blends to pre-alloyed powders with combinations of ductile-ductile or ductile-brittle or brittle-brittle materials.

Unlike many of the above methods, mechanical attrition produces its nanostructures not by cluster assembly but by the structural decomposition of coarser-grained structures as the result of severe plastic deformation. This method has become popular in making nanocrystalline materials because of its simplicity, the relatively inexpensive equipment (on the laboratory scale) needed, and the applicability to essentially all classes of materials. The major advantage often achieved is the possibility for easily scaling up to tonnage quantities of material for various applications. Similarly, some serious problems usually cited are, (i) contamination from milling media and/or atmosphere [7]; careful attention can reduce/eliminate this problem, and (ii) the need (for structural applications) to consolidate the powder.

### **2.2.2 Developments in Mechanical alloying (MA)**

MA is a capable process to synthesize nanostructured materials presenting improved properties compared to conventional coarse-grained materials [8].

### **2.2.3 Process Variables**

Mechanical alloying is a complex process and hence involves optimization of a number of parameters or variables to achieve the desired product phase and/or microstructure. Some of the important parameters which have an effect on the final constitution of the powder are:

- Type of mill
- Milling container
- Milling speed
- Milling time
- Type, size, and size distribution of the grinding medium
- Ball-to-powder weight ratio
- Extent of filling the vial
- Milling atmosphere
- Process control agent
- Temperature of milling

All these process variables are not completely independent. For example, the optimum milling time depends on the type of mill, size of the grinding medium, temperature of milling, ball-to-powder ratio, etc.

#### **Type of mill**

There are a number of different types of mills for conducting MA. Depending on the requirements, type of product to be produced, quantity of the product and facilities available, the mill is chosen. Most commonly, however, the SPEX shaker mills are used for alloy screening purposes. The Fritsch Pulverisette planetary ball mills or the attritor mills are used to produce large quantities of the milled powder. Specially designed mills are used for specific applications.

#### **Milling container**

Hardened steel, tool steel, hardened chromium steel, tempered steel, stainless steel, WC-Co, WC- lined steel and bearing steel are used for the grinding vessels. Care should be taken to confirm that there is no cross contamination from milling media and vials. On the other hand, if the two materials are the same, then the chemistry may be altered unless proper precautions are taken to compensate for the additional amount of the element incorporated into the powder.

### **Milling speed**

The efficiency of milling increases with increase in speed. However, it shouldn't exceed critical speed of the mill. Above a certain critical speed, the balls would be pinned to the inner walls of the vial and would not fall down to exert any impact force. Therefore, the maximum speed should be just below this critical value. Another limitation to the maximum speed is the temperature rise during milling. This may be advantageous in some cases where diffusion is required to promote homogenization and/or alloying in the powders. But, in some cases, this increase in temperature may be a disadvantage because the increased temperature accelerates the transformation process and results in the decomposition of supersaturated solid solutions or other metastable phases formed during milling. For this work 1750 rpm milling speed is chosen.

### **Milling time**

The time of milling is the most important parameter. Normally the time is so chosen as to achieve a steady state between the fracturing and cold welding of the powder particles. The time required varies depending on the type of mill used, the intensity of milling, the ball-to-powder ratio, and the temperature of milling. The level of contamination increases with milling time and some undesirable phases form. Therefore, it is desirable that the powder is milled just for the required duration and not any longer. Milling time of 25 h is normally chosen for this work.

### **Grinding medium**

Hardened steel, tool steel, hardened chromium steel, tempered steel, stainless steel, WC-Co, and bearing steel are the most common types of materials used for the grinding medium. It is always desirable to have the grinding vessel and the grinding medium made of the same material as the powder being milled to avoid cross contamination. Stainless steel was used as grinding medium for present study during mechanical milling. The size of the

grinding medium also has an influence on the milling efficiency. It has been reported that a combination of large and small size balls during milling minimizes the amount of cold welding and the amount of powder coated onto the surface of the balls.

### **Ball-to-powder weight ratio (BPR)**

The ratio of the weight of the balls to the powder (BPR), sometimes referred to as charge ratio (CR), is an important variable in the milling process. The minimum BPR ranges from as low as 1:1 to as high as 220:1. In general ratio of 10:1 is most commonly used while milling the powder in a small capacity mill like a SPEX mill. However, when milling is conducted in a large capacity mill, like an attritor, a higher BPR of up to 50:1 or even 100:1 can be used. The ball to powder weight ratio of 10:1 was taken for present study.

### **Extent of filling the vial**

Since alloying among the powder particles occurs due to the impact forces exerted on them, it is necessary that there is enough space for the balls and the powder particles to move around freely in the milling container. Hence, the extent of filling the vial with the powder and the balls is important. Thus, care has to be taken not to overfill the vial; generally about 50% of the vial space is left empty.

### **Milling atmosphere**

Different atmospheres have been used during milling for specific purposes. Nitrogen or ammonia atmospheres have been used to produce nitrides. Hydrogen atmosphere was used to produce hydrides. The presence of air in the vial has resulted in to producing oxides and nitrides in the powder, especially when the powders are reactive in nature. Thus, care has to be taken to use an inert atmosphere during milling.

### **Process control agents**

A process control agent (PCA) is added to the powder mixture during milling to reduce the effect of cold welding. The nature and amount of the PCA used and the type of powder milled would determine the final size, shape, and purity of the powder particles. Use of a high amount of the PCA normally reduces the particle size by 2-3 orders of magnitude. The amount of the PCA depends upon the factors : (a) cold welding characteristics of the powder particles, (b) chemical and thermal stability of the PCA, and (c) amount of the powder and grinding medium used. Some important PCAs include stearic acid, hexane,

Toluene, methanol, and ethanol. Toluene was used as a process control agent for present investigation.

### **Temperature of milling**

There have been conflicting reports on the formation of an amorphous phase as a function of the temperature of milling. Amorphization during MA involves formation of microdiffusion couples of the constituent powders followed by a solid-state amorphization reaction. Lower milling temperatures are expected to favour amorphization. However, both increased and decreased kinetics have been reported. Milling was carried out in room temperature for present study.

### **2.2.4 Mechanism of alloying**

During milling when two hard balls collide, a very small amount of powder is entrapped in between them. Typically, around 1000 particles are trapped during each collision (Fig. 2.1). The impact force deforms the powder particles plastically leading to work hardening and fracture. The new surfaces created enable the particles to weld together and this leads to an increase in particle size in case of ductile-ductile or ductile-brittle combination of materials.

At this stage, the composite particles have a characteristic layered structure (Fig. 2.3) consisting of various combinations of the starting constituents. With continued deformation, the particles get work hardened and fractured/fragmented of fragile flakes. At this stage, the tendency to fracture dominates over cold welding. Due to the continued impact of grinding balls, the structure of the particles gets steadily refined, but the particle size continues to be the same after certain duration of milling. Steady-state equilibrium is reached when a balance is achieved between the rate of cold welding and the rate of fracturing. At this stage each particle contains substantially all of the starting ingredients in the same proportion of initial composition.

During MA, a variety of crystal defects such as dislocations, vacancies, stacking faults, and increased number of grain boundaries are introduced. The defects such as dislocations, vacancies, stacking faults etc., which are introduced during MA, enhance the diffusivity of solute elements into the matrix. The diffusion distance is also reduced due to refinement of the microstructure. Moreover, the slight rise in temperature of the material

during milling also aids the diffusion. Consequently, true alloying takes place amongst the constituent elements [9].

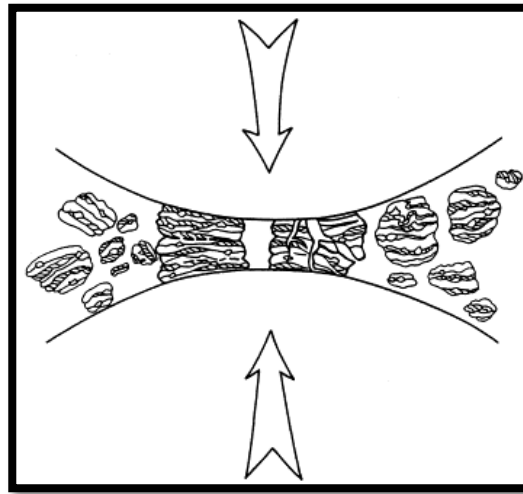


Fig 2.1: Ball-powder-Ball collision of powder mixture during MA

In planetary ball mill, both the centrifugal force produced by the vials rotating around their own axes and that produced by the rotating support disk act on the vial contents consisting of material to be ground and the grinding balls. Now since the vials and the supporting disk rotate in opposite directions, the centrifugal forces alternately act in like and opposite directions. As a result, the grinding balls run down the inside wall of the vial- the friction effect, followed by the material being ground and grinding balls lifting off and travelling freely through the inner chamber of the vial and colliding against the opposing inside wall -the impact effect (Fig. 2.2).

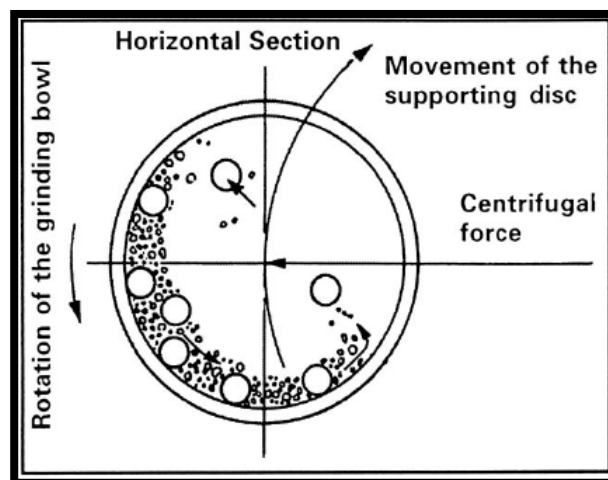


Fig. 2.2: Schematic diagram depicting the ball motion inside the ball mill

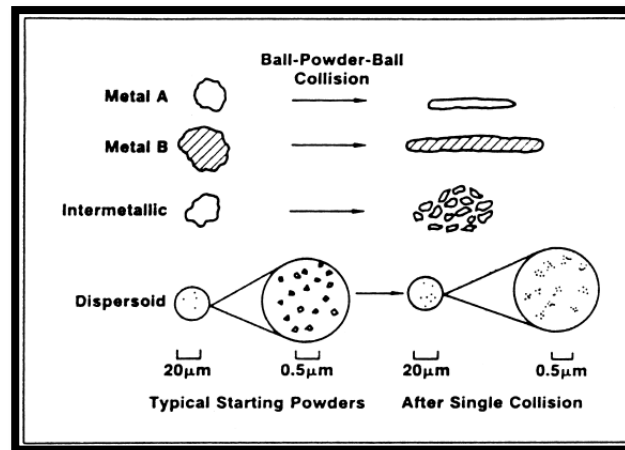


Fig 2.3: Layered structured formed during mechanical alloying.

### 2.2.5 Advantages of Mechanical Milling (MM)

MM is a simple and economically feasible process with many important technical advantages.

- Usually, we make alloys by melting together the components, whereas, Mechanical alloying involves the synthesis of materials in solid state by high-energy ball milling.
- Bulk material with dimension larger than rapid solidification process (RSP) can be produced by MM.
- Synthesis of novel alloys is possible, e.g., alloying of normally immiscible elements, which is not possible by any other technique like RSP. This is because MM is a completely solid state processing technique and hence the limitations imposed by phase diagrams don't apply here.
- Extended solid solubility was achieved by MM in some alloy system. This technique can be used to induce chemical displacement reactions in powder mixtures at room temperature or at much lower temperature than normally required to synthesize pure metals.
- MM can be used for the refinement of the matrix microstructure down to nanometer range. These nanostructures obtained not by clustered assembly but by the structural decomposition of coarser grained structures as the result of severe plastic deformation.



- Amorphous phase formation is one of the most frequently reported phenomena in mechanically alloyed powder mixtures.

### 2.3 Mechanical Alloying to prepare Iron based Nanocrystalline

Mechanical deformation under shear conditions and high strain rates ( $\sim 10^1$ - $10^4$ ) leads to the formation of nanostructures within powder particles, thin foils or at the surface of metals and alloys exposed to friction induced wear conditions. Solid state (mechanical) alloying beyond the thermodynamic limit can lead to the formation of amorphous metallic materials as observed for a broad range of alloys. During mechanical alloying metals with FCC structure are inherently more ductile and often exhibit a stronger tendency to adhere to the container walls and to sinter into larger particles often several millimetres in diameter. More milling time leads to more strain which implies peak broadening in the x-ray diffraction patterns. The major obstacles for the use of intermetallic compounds as structural materials are their low ductility and toughness at ambient temperature and, in some cases, insufficient strength and creep resistance at high temperatures. While macro alloying or micro alloying has been successful in increasing ductility in specific intermetallic [10].

Previously MA was generally conceived for the production of dispersion strengthened super alloys, is nowadays used for synthesizing a wide range of materials including intermetallics. MA is a solid state, dry milling process that leads, through micro sandwich morphology, to the ultimate mixing of elemental powders and eventually to alloy formation [11].

F. Tehrani et al. studied on the effect of particle size of iron powder on  $\alpha$  to  $\gamma$  transformation in the nanostructured high nitrogen Fe–18Cr–10Mn–4Mo stainless steel with two different particle sizes and found that Variations of grain size and internal lattice strain versus milling time, for both iron particle sizes, showed that the critical ferrite grain size for austenite nucleation is less than 10 nm [12]. While synthesizing alloy of Fe–Al–Ni by mechanical alloying F. Hadeef et al. found that BCC structured alloy of two different phases with same crystal size but different lattice parameters, proportions and microstrains were developed named as  $\alpha_1$ -Fe(Al, Ni) and  $\alpha_2$ -Fe(Al, Ni). The later one disappears after 4 h and a chemically homogenised structure of  $\alpha_1$ -Fe (Al, Ni) lefts behind [13]. By mechanical alloying the solubilities in the Fe–Cu system can be largely extended. It holds good mostly for the single fcc-structure [14].

In the Fe-based powder, with increasing milling time the grain size of the MA powder decreases; however, the decrease in particle size is not linear with milling time. Milling time of 144 h. and more leads to serious cold-welding. The relative density of the as-sintered alloys is influenced by the particle size of the powders before sintering. The coarse particles lead to a low density in the sintered alloys. In the elongated particles the micro hardness is higher than that in the equiaxed grains, the main causes are higher density of the precipitated phase and the larger residual strain [13].

## **2.4 Grain growth of Iron based Nanocrystalline prepared by Mechanical alloying**

The main objective of mechanical alloying is to produce nanocrystalline material. It also helps in extending solid solution limit in some alloy systems so that properties of the alloy can be increased [16]. Hence it is very important to study the grain growth behaviour of solid solutions prepared by mechanical alloying as, while going through different physical or thermal processing routes the grain growth occurs. The grain growth mechanism of nanocrystalline materials is different than polycrystalline materials [15]. This can be analysed by considering the grain size of a poly crystalline material is very small.

The more is the grain boundary the more is the energy associated with it. So to achieve a stable state, the system leads to reduce the grain boundary by increasing the grain size. The rate of the grain growth shows linear relation with the size of the grain and is inversely proportional [16,17].

$$dD/dt = k/D \quad (1)$$

Where D is the mean grain diameter after an annealing time t and k is the temperature (T) dependent rate constant.

The integration of the above equation leads to give the grain size D, at t = 0 yields, under ideal conditions.

$$D^2 - D_0^2 = kt. \quad (2)$$

Mostly for high purity metals at high homologous temperatures the grain growth takes place in a parabolic manner. For practical purposes, the most widely used empirical time constant  $n \leq 0.5$ . By the below equation grain growth under isothermal condition can be described [18].

$$D^{1/n} - D_0^{1/n} = k't \text{ or } D = (k't + D_0^{1/n})^n \quad (3)$$

Pinning forces can affect grain growth in a way that the grain boundary migration may stop before the curvature is completely eliminated. The rate of growth is then proportional to the difference between the curvature of the actual grain size at the given annealing time ( $1/D$ ) and the curvature of the grain size that corresponds to the limiting curvature where the growth stops ( $1/D_m$ ):

$$dD/dt = k(1/D - 1/D_m) \quad (4)$$

The final form from this analysis is [8]:

$$(D_0 - D)/D_m + \ln[(D_m - D_0)/(D_m - D)] = kt \quad (5)$$

Where  $D_m$ , is the maximum grain size that results due to the pinning force;  $k$  is here given in the units [ $s^{-1}$ ], but can be expressed in the units [ $nm^2/s$ ] as  $K = kD_m$ . The rate constant  $k$  (or  $k'$ ) can be expressed in an Arrhenius-type equation:

$$k = k_0 \exp\{-Q/RT\} \quad (6)$$

Where  $Q$  is the activation energy for isothermal grain growth and  $R$  is the molar gas constant.

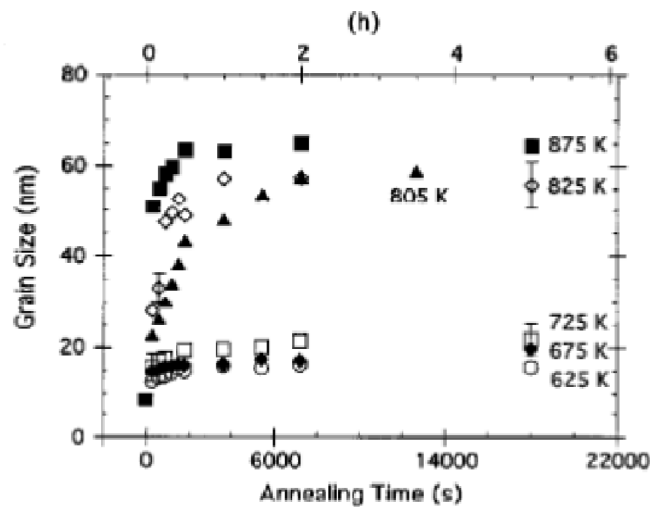


Figure1: Grain size as measured by XRD as a function of annealing time for nanocrystalline Fe annealed at various temperatures between 625 and 875 K [15].

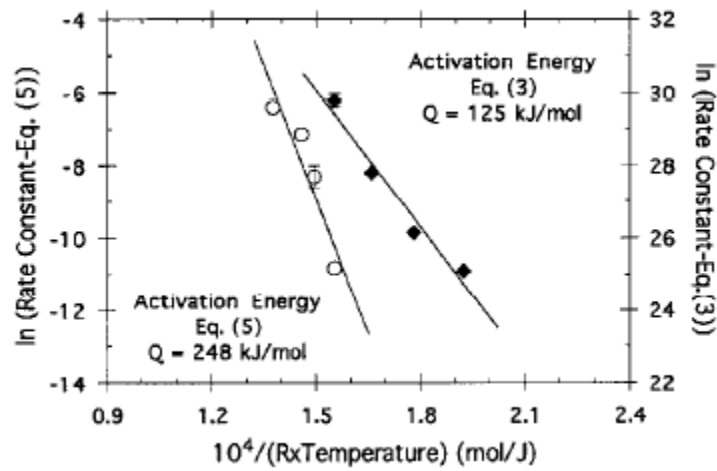


Figure2: Arrhenius plot of grain growth data of nc Fe analysed according to equations (3) and (5). The slope of the linear fit in the plot is used to deduce the activation energy [15].

From the above figure activation energy  $Q$  is 125 kJ/mol without considering the pinning force for for an exponent  $n = 0.083$  and  $Q = 248$  kJ/mol considering pinning force. From DSC the obtained value of  $Q$  is  $224 \pm 25$  kJ/mol [15].

## 2.5 Grain growth stabilization

Mechanical properties like hardness, coercitivity, diffusion processes are greatly varied due to microstructure. Grain growth behaviour of different metals and alloys depends upon a number of important variables, which can be defined in terms of mathematical expressions. Titanium, vanadium, zirconium, niobium or aluminium in steels can be used as grain growth stabilizers. This improves quality of structural steel for variety of application. Many researchers have developed both static and dynamic models to minimize grain growth by second phase particles [19,20].

The variation in the particle radius ( $r$ ) and volume fraction of precipitates is a function of time and temperature can be represented by Kinetic models. Independent work of Lifshitz and Slyovoz [21] and Wagner [22] reveals how particles coarsen and found that, The kinetics are normally controlled by volume diffusion through the matrix provided the grain boundaries should have a negligible influence on the process. Time dependence of the mean particle radius ( $r$ ) at steady state given by them is

$$r^3 - r_0^3 = \frac{8\gamma D_m C_m (V_m')^2}{9RT} t \quad (3)$$

Equation (3) can be applied to continuous heating and cooling. In a more general form this is represented by Lon et al [23].

$$r^3 - r_0^3 = \frac{C_1 t}{T} \exp\left(-\frac{Q_s}{RT}\right) \quad (4)$$

Where  $r_0$  is the initial particle radius,  $V_m'$  molar volume of precipitate per mole of diffusate ( $\text{m}^3/\text{mol}$ ),  $t$  is time (s),  $r$  particle radius (m,  $\mu\text{m}$  or nm),  $D_m$  is element diffusivity ( $\mu\text{m}^2/\text{s}$ ,  $\text{mm}^2/\text{s}$  or  $\text{m}^2/\text{s}$ ),  $C_m$  is concentration of solute in matrix ( $\text{mol}/\text{m}^3$  or wt. %),  $R$  is universal gas constant ( $8.314 \text{ J/K mol}$ ),  $T$  is temperature ( $^\circ\text{C}$  or K). The equation (3) suffers from a number of simplifying assumptions.

With the excess amount of solute on the boundary the effective grain-boundary free energy  $\gamma$  per unit area varies according to the Gibbs interface equation

$$d\gamma = -\Gamma d\mu \quad (5)$$

Where  $\Gamma$  is the solute atom excess (mol/area) on a grain boundary and  $\mu$  is the chemical potential of the solute (energy/mol) [24]. Therefore if solute segregation  $\Gamma = 0$ , then free energy change will be  $d\gamma = 0$ .

K.A. Darling et al. found that the addition of Ni as segregate to Fe did very little to stabilize against grain growth while Zr had a more significant effect than Ta. Grain growth behaviour is abnormal. The value of abnormality increases with temperature and decreased with solute type as Ni, Ta and Zr respectively [25].

Another method of stabilization is particle pinning. Presence of second phase particles leads to pinning of grain domain boundaries as a result of which an upper limit to grain size during grain growth (although not necessarily recrystallization) is set. Once a boundary has intersected with a particle, a certain amount of boundary area is removed from the system. In order for the boundary to move off the particle, the “missing area” must be re-created. This restoration of boundary area requires an energy increase. Through the principle of virtual work, this requires a force.

Zener’s assumption was that the boundaries can be assumed to intersect randomly with the particles. The fraction of particles with radius  $r$  and volume fraction ( $f$ ) that intersect unit area of a random oriented section plane is  $3f/2\pi r^2$ . Drag pressure is the product of maximum force per particle and the number per unit area of boundary.

$$P_{\text{drag}} = \pi\gamma r * 3f/2\pi r^2 = 3f\gamma/2r \quad (6)$$

The effect of the presence of fine particles is to slow down, and eventually stop grain growth [8].

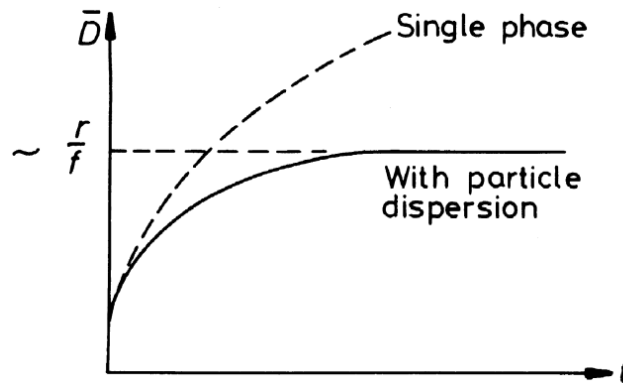


Figure 1: Effect of second phase particles on grain growth

The above equation (6) given by Zener based on the assumption that pinning force occurs due to single second phase particle and shape of the particle is spherical so interface between a particle and matrix is incoherent [26]. While shape of the particle may be spherical, needle like, plate shaped or cuboidal [27]. N. Moelans et al. found that in pinning columnar grain boundaries nonspherical particles shows better result when the larger side of the columnar grain boundaries are oriented perpendicular to the plane of the film [28]. According to A. Harun et al. pinning geometry of a catenoid of revolution first calculated by Hellman and Hillert, is the minimum energy configuration [29]. K chang et al. found that ellipsoidal particles of eccentricity more than 0.35 are more effective in pinning than cuboidal particle and for eccentricity less than 0.35 cuboidal particles shows better result in pinning [27].

Grain growth can be minimised by rapid solidification of liquid melt. Zheng Chen et al. used this technique to study the grain growth in the undercooled Fe-4 at.% Cu in a controlled way. They proposed a model by which alloy of iron and copper can be produced in nano scale. The model of grain growth is a combination of kinetic-controlled process, a transition from kinetic mechanism to thermodynamic-mechanism and purely thermodynamic-controlled process [30]. In the above process the effective grain boundary energy is reduced. The driving force can be eliminated by thermodynamic approach, which requires a negative free energy change for segregation of solute atoms from solid solution to grain boundaries [31].

Molinari et al. studied the Role of lattice strain on thermal stability of a nanocrystalline Fe-Mo alloy. They found that crystallite size and average dislocation density is a function of temperature and silica nanoparticles in Fe-Mo alloy decrease the domain size and simultaneously increase the grain-boundary strain in the as-milled powder. Grain-boundary strain stabilizes the domain size. Whose effect is greater than that of the Zener stresses due to grain boundary nanopores and grain boundary silica particles. With the release in certain amount of Zener strain grain growth starts [32].

J. Svejcar et al. investigated different grain growth inhibitors by Energy Dispersive X-RAY analysis. According to their study in a 3% Si-Fe alloys containing various proportions of silicon, sulphur, manganese and iron or aluminium and the smallest particles always contains silicon as the main component which has size of 20-50 nm [33].

Heather A. Murdoch et al. in terms of alloy thermodynamic parameters established a “nanostructure stability map”. They developed a model to Stabilize binary nanocrystalline alloys against grain growth and phase separation. The map is given below

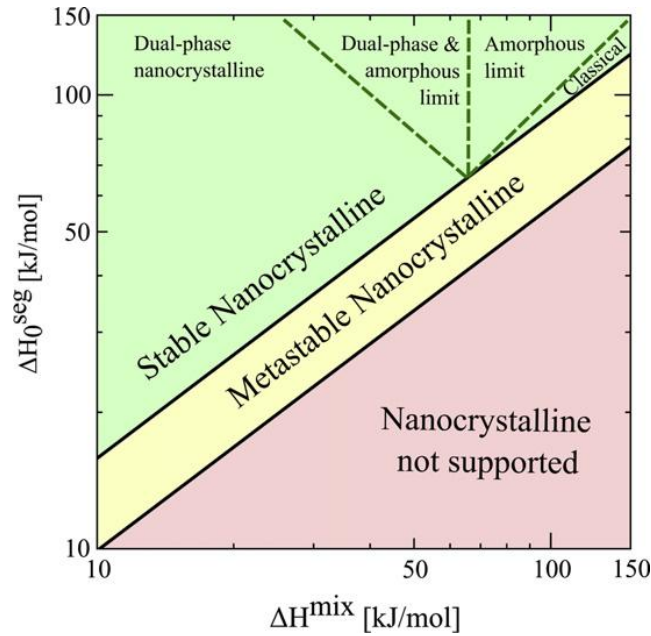


Figure 2: Nanostructure stability map, presenting delineated regions of stability (green), metastability (yellow) and no stability (red) in binary alloys as a function of their enthalpies of mixing and segregation. This map is calculated for a fixed dimensionless temperature of  $0.35T_{\text{cr}}$  [34].

From the above figure it is clear that  $\Delta H_0^{\text{seg}}$  should be higher than  $\Delta H^{\text{mix}}$  to get stable nanocrystalline. Different stable nanocrystallines can be obtained which are stable having compositions greater than bulk solubility limit. In the metastable region nanocrystalline are possible with stable grain growth while occurrence of macroscopic phase separation can be observed [34].



## 2.5 Hardness

Hardness is a measure of how resistant solid matter is to various kinds of permanent shape change when a force is applied. There are three main types of hardness measurements: scratch, indentation, and rebound. Scratch hardness is the measure of how resistant a sample is to fracture or permanent plastic deformation due to friction from a sharp object. Indentation hardness measures the resistance of a sample to material deformation due to a constant compression load from a sharp object; they are primarily used in engineering and metallurgy fields. Rebound hardness, also known as dynamic hardness, measures the height of the "bounce" of a diamond-tipped hammer dropped from a fixed height onto a material. This type of hardness is related to elasticity [35,36]

Many researchers have worked on nanocrystalline materials and studied their behaviour towards microhardness [37-41] and their result shown gives contradicting picture towards relationship between grain sizes and microhardness, as according to some researchers with decrease in grain size microhardness increases [37-40] while according to others microhardness decreases with decreases in grain size [39,40]. This can be explained by different metallurgical aspects. According to Hall-Petch equation the relationship between grain sizes and microhardness in coarse-grained materials is

$$H_v = H_0 + k d_1^{-1/2} \quad (1)$$

Where  $H_v$  is the hardness,  $H_0$  and  $k$  are constants, and  $d_1$  is the average grain size. The above equation shows that with decrease in grain size microhardness increases. Nieman et al. [3] reported that nanocrystalline palladium samples (20 nm) show a four-fold increase in hardness compared to coarse-grained (100  $\mu\text{m}$ ) palladium and a doubling in hardness for nanocrystalline copper samples (25 nm) over coarse-grained (50  $\mu\text{m}$ ) copper [37]. The above equation (1) has limitations because the strength does not increase indefinitely with decreasing grain size as the strength value cannot exceed the theoretical strength, i.e., the strength of a perfect whisker. Rather fine grain below a certain limit may decrease the strength by softening the material. This can be defined due to Inverse Hall-Petch relation.

Mechanical milling increases hardness up by the mechanism of grain refinement strengthening. Annealing reduces hardness and induces grain growth. The Vickers hardness of nanocrystalline grains shows less interaction towards Hall-Petch equation rather than coarse-grained powders annealed at high temperatures [39].

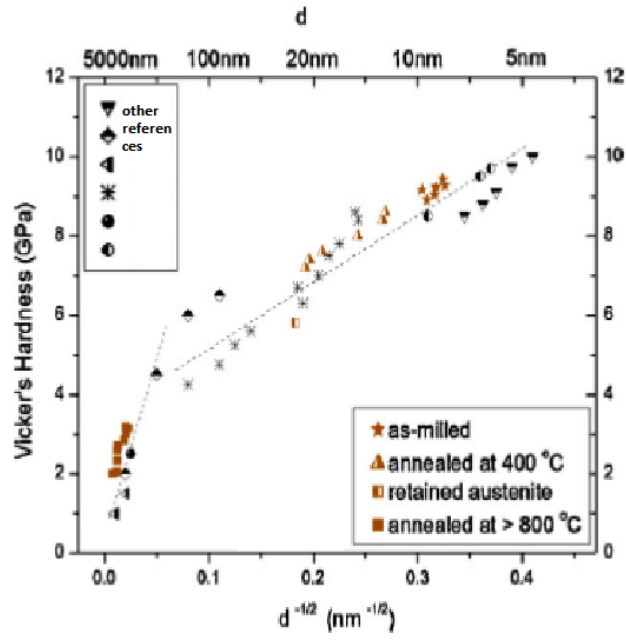


Figure 1: Hall–Petch plot of the hardness of as-milled, annealed nanocrystalline and annealed coarse-grained iron and iron–nickel alloys [37].

### 3. Experimental

In this section, we would see the various experimental procedures that were carried out during the project starting from mechanical alloying in spex mill till analysing data from XRD.

#### Materials used:

1. Iron powder (100  $\mu\text{m}$ )
2. Yttrium powder (in atom percentage)

#### High energy ball Mill

Milling was done in shaker mill (SPEX 8000). Stainless steel balls were used as the milling media in a stainless steel vial and the ball mill was rotated at 1750 rpm. Milling atmosphere was made inert with Argon gas. The ball to powder ratio used for milling was 10:1.



Fig 3.1 : High energy shaker mill ( SPEX 8000)

Three different compositions were prepared. Each sample was milled for 1500 minutes.

1. Sample A- pure iron(Fe)
2. Sample B- Fe-0.25 atom % Y
3. Sample C- Fe-0.50 atom % Y

$$\text{Atom \% of Y} = \frac{\frac{\text{Wt \% Y}}{\text{Atomic wt of Y}}}{\frac{\text{Wt \% Y}}{\text{Atomic wt of Y}} + \frac{\text{Wt \% Fe}}{\text{Atomic wt of Fe}}}$$

### **Compaction by pelletization:**

The powdered samples were compacted in form of pellets in pellet pressing machine (Carver pellet pressure machine) to prevent oxidation of powdered sample, under load of 6.5 tonnes for a dwell time of 90 seconds. For each pellet, 0.5 grams(approx.) of sample powder is taken and binder used was PVA(Polyvinyl acetate). Die punch combination used was of 7mm dia and made up of tungsten carbide.



Fig 3.2 : Carver pellet pressure machine

### **Heat Treatment:**

The pellets were annealed at different temperature under inert atmosphere of pure argon. The pellets were heated at a rate of 5°C/Min and were held at the annealing temperature for 1 hour and then cooled to room temperature. The furnace used was tubular furnace having maximum temperature range of 1750°C.

The pellets were annealed at 500°C, 700°C, 900°C & 1200°C.



Fig 3.3 : Tubular furnace used for annealing

### **X-ray Diffraction:**

X-ray diffraction of the as milled samples as well as annealed pellets was carried out in a PANalytical Xpert high-resolution X-ray diffractometer. The data was analyzed for phases present, crystallite size and lattice strain.

### **Microhardness measurement:**

Microhardness testing of the annealed samples and as milled samples is done using Vickers microhardness testing machine with a magnification of 50X, using load of 50gf for a dwell time of 15 seconds. The formula used to get the hardness was

$$H.V = \frac{1.854 \times P}{L \times L}$$

## 4. Result and Discussions

### 4.1 Vickers' microhardness test results:

Magnification = 50 X

Load=50 gf

Sl no.	Sample	Annealing Temp.( °C)	Avg. Micro hardness (HVN)
1.	A (pure Fe)	As milled	813.78
		500°C	680.14
		700 °C	360.98
		900 °C	474.12
		1200 °C	270.6
2.	B (Fe-0.25atom% Y)	As milled	936.48
		500°C	858.44
		700 °C	736.48
		900 °C	672.5
		1200 °C	389.6
3.	C (Fe-0.5atom% Y)	As milled	1012.8
		500°C	909.94
		700 °C	892.26
		900 °C	716.9
		1200 °C	553.32

Table 4.1 : Microhardness values of samples with varying composition and annealing temperature

## 4.2 Structural Characterization of Milled Samples

The structural characterizations of the mechanically milled powder samples was carried out by XRD.

### 4.2.1 XRD analysis

XRD is a very good characterisation technique used to determine the crystallite size and lattice strain of different materials.

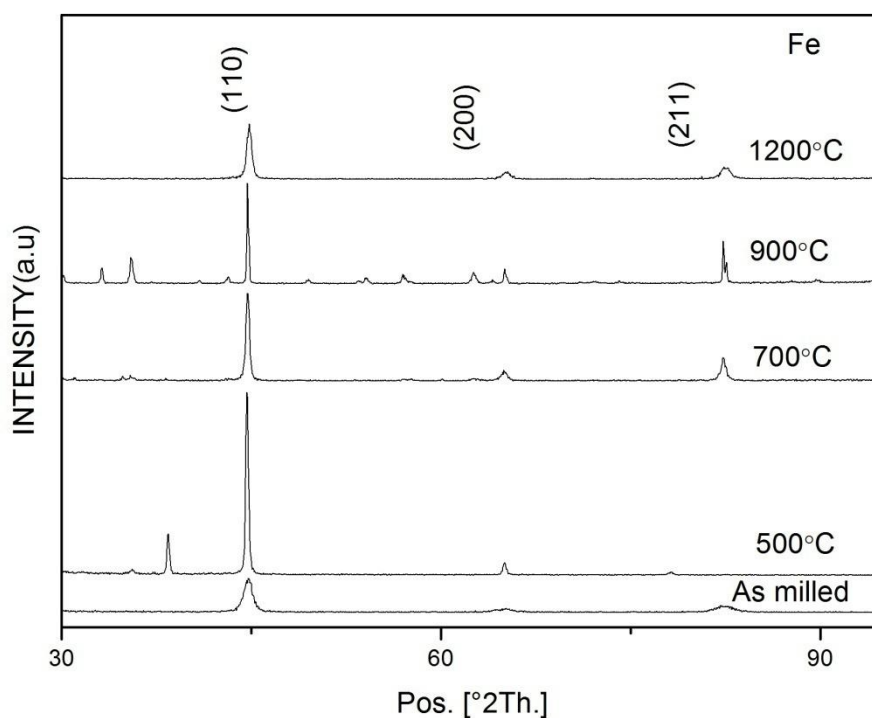


Figure 4.1: XRD pattern of pure Fe at different temperature

The above figure shows XRD pattern of pure Fe annealed at different temperatures. The XRD peaks of the samples are (110), (200) and (211). In the above figure the lattice strain is more for wider peaks which will be discussed later.



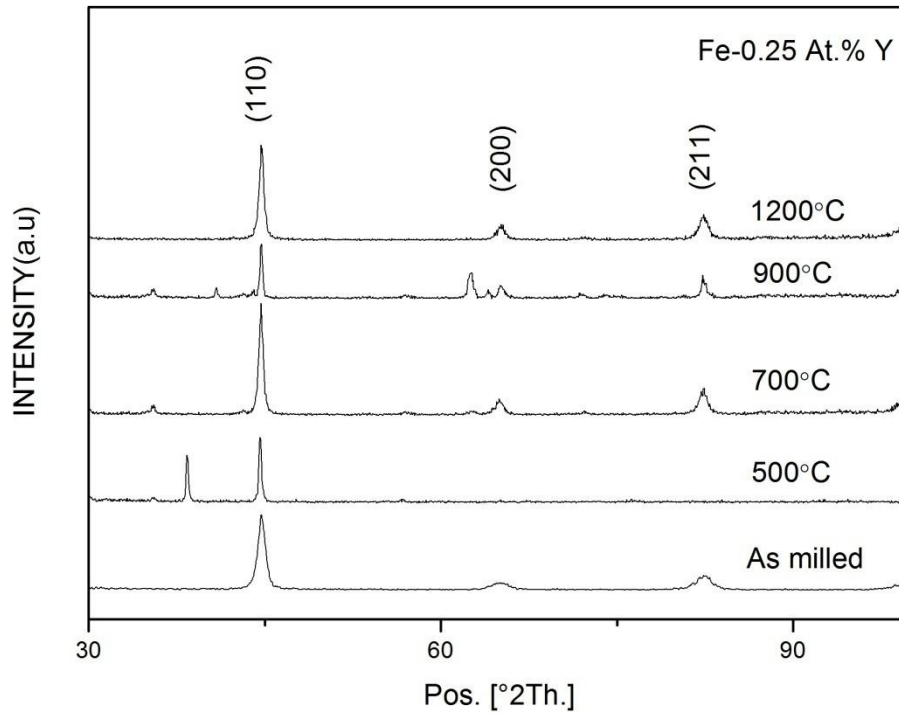


Figure 4.2: XRD pattern of Fe-0.25 wt.% Y at different temperature

The above figure shows XRD pattern of Fe mechanically alloyed with 0.25% Y for 1500 minutes, annealed at different temperatures. The XRD peaks of the samples are (110), (200) and (211). A high amount of broadening is observed in the as milled condition which shows the presence of large lattice strain.



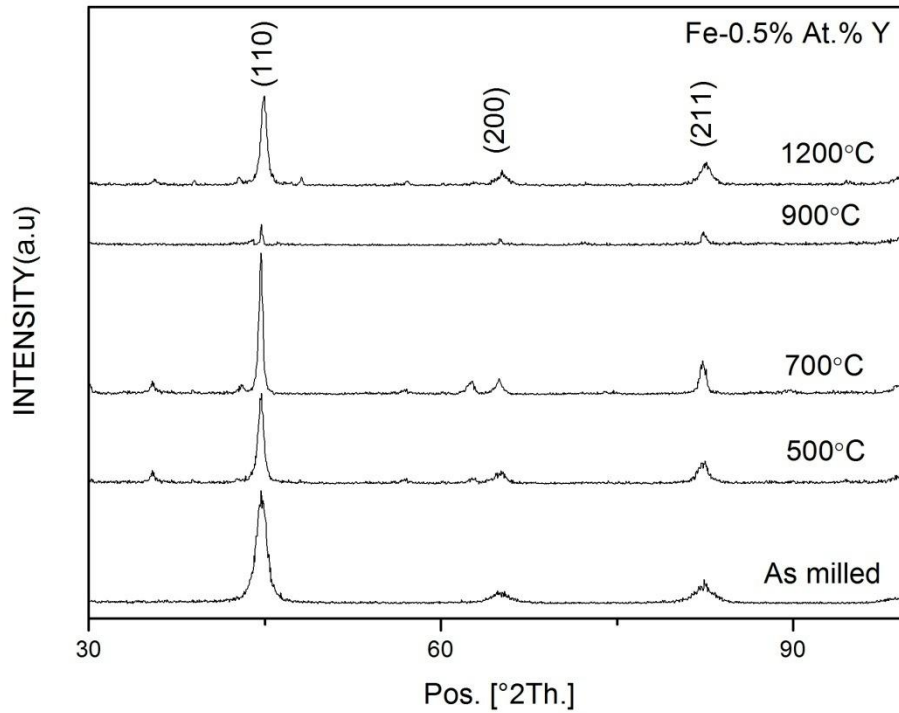


Figure 4.2: XRD pattern of Fe-0.5 wt.% Y at different temperature

The above figure shows XRD pattern of Fe mechanically alloyed with 0.50% Y for 1500 minutes, annealed at different temperatures. The XRD peaks of the samples are (110), (200) and (211). Peak broadening is observed in the as milled condition and annealing at 1200°C.

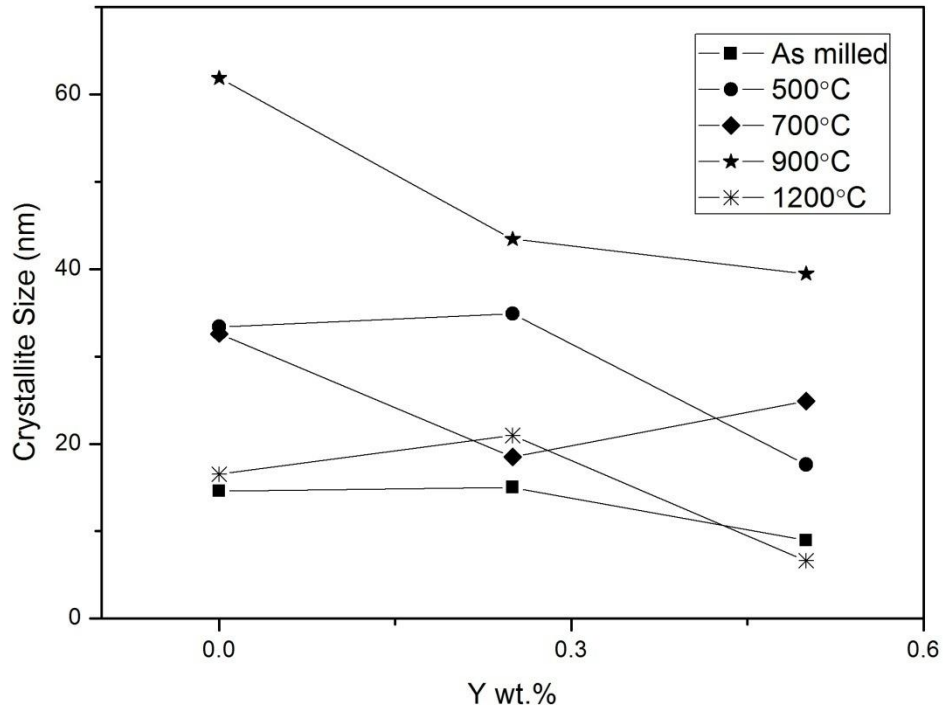


Figure 4.4: Variation of crystallite size at different temperatures with addition of yttrium in Fe

The crystallite size is calculated by Scherrer's formula: 
$$d = \frac{0.9\lambda}{B \cos \theta}$$

The above figure displays the variation of crystallite size with Y content and annealing temperature as analysed from the XRD peaks plot obtained. In the as milled state, the crystallite size remains nearly constant till 0.25 % Y but then decreases. The crystallite size is observed to increase gradually up to 0.25 atom % Y and then decreases in samples annealed at 500°C, 1200°C. In case of samples annealed at 900°C, the crystallite size decreases progressively with increase in % Y. On annealing at 700°C, the crystallite size first decreases till 0.25 % Y and then increases. The crystallite sizes of samples annealed at 900°C are found to be larger in comparison to corresponding values at other temperatures. The maximum crystallite size is obtained at pure Fe sample annealed at 900°C as 61.85 nm and a minimum of 6.62 nm at 1200°C.

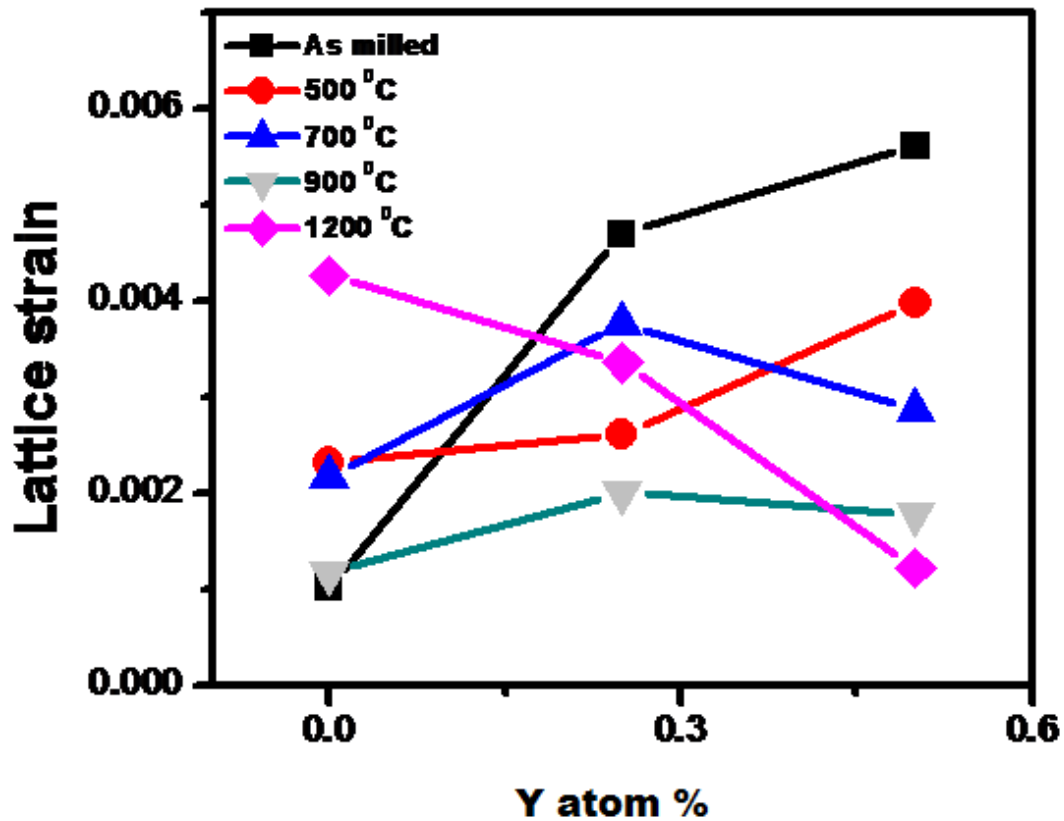


Figure 4.5: Variation of Lattice Strain at different temperatures with addition of yttrium.

The lattice strain is calculated as :  $\mu = \frac{B}{4\tan\theta}$

The above plot shows the variation of lattice strain with atom % Y and temperature of annealing. The more the broadening of peaks, higher is the lattice strain. The data based on the broadening of peaks observed in the XRD plot is analysed. As we see, the lattice strain increases progressively with increase in the %Y in as milled condition and in samples annealed at 500 °C. Hence the yttrium addition makes a positive contribution to lattice strain causing solid solution straining. In case of samples annealed at 700°C and 900°C, the lattice strain first increases up to 0.25 %Y and then decreases. The lattice strain is found to decrease continuously with % Y when annealed at 1200 °C which shows that Y addition does not have any significant effect when annealing is done at high temperature . A maximum lattice strain is observed in as milled condition of Fe-0.5 atom% Y i.e. 0.0056.

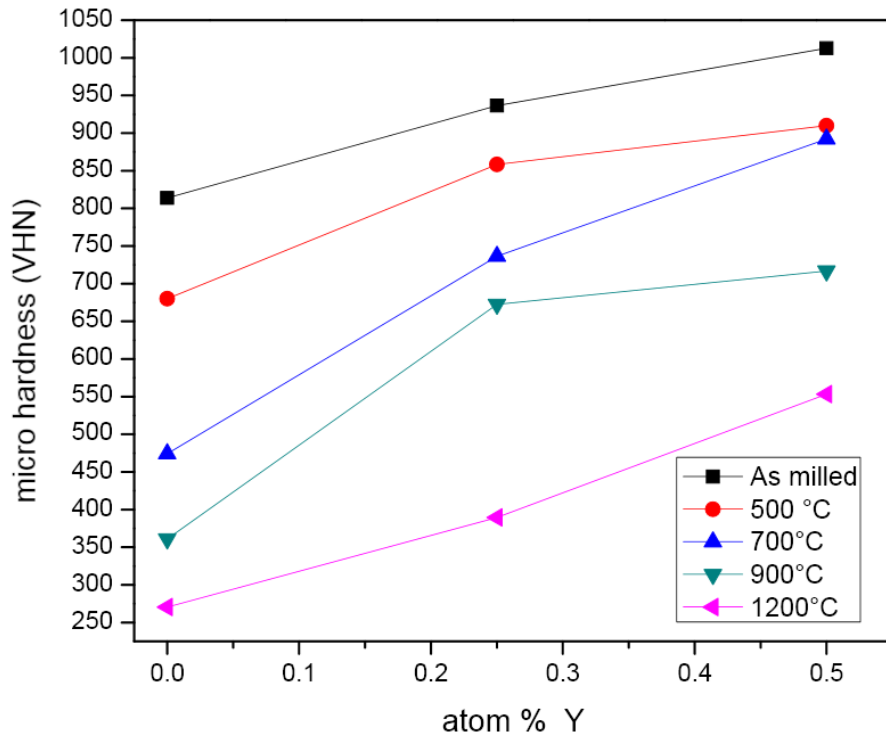


Figure 4.6: Variation of Micro hardness at different temperatures with addition of yttrium.

The above figure displays the variation of micro hardness value obtained, with the %Y and annealing temperature. It is extremely clear that, when we consider samples annealed at identical temperature, the microhardness increases with increase in %Y. With increase in annealing temperature, the hardness decreases as expected. The maximum micro hardness of 1012.8 VHN is obtained in the 0.5 atom % Y sample in as milled condition while minimum of 270.6 VHN is found at 1200°C in pure Fe sample. Hence , we found that the addition of Yttrium in minute amounts enhances the hardness of Fe nanostructures.

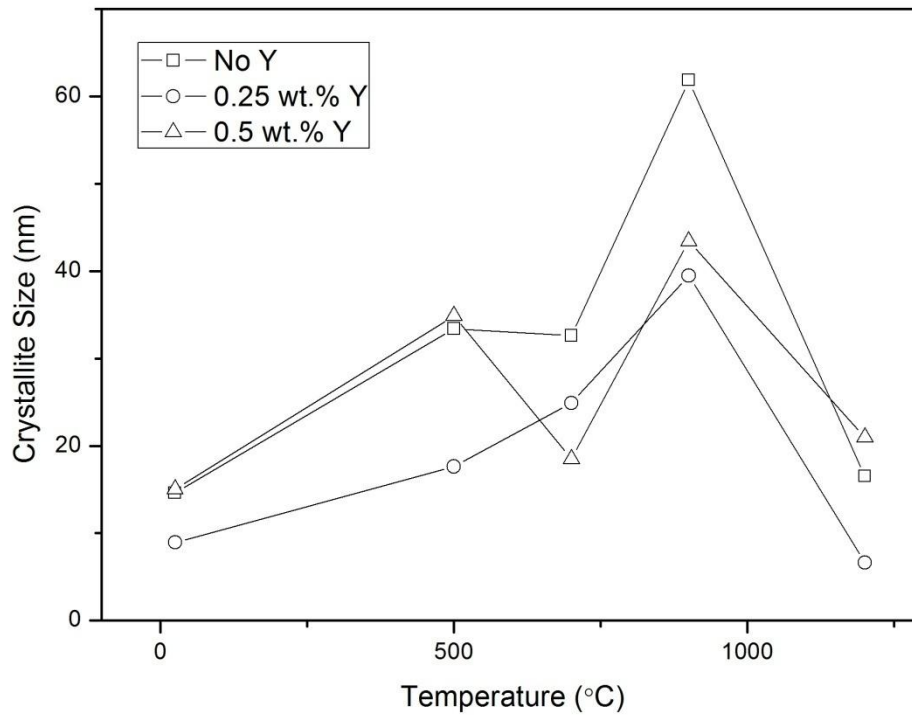
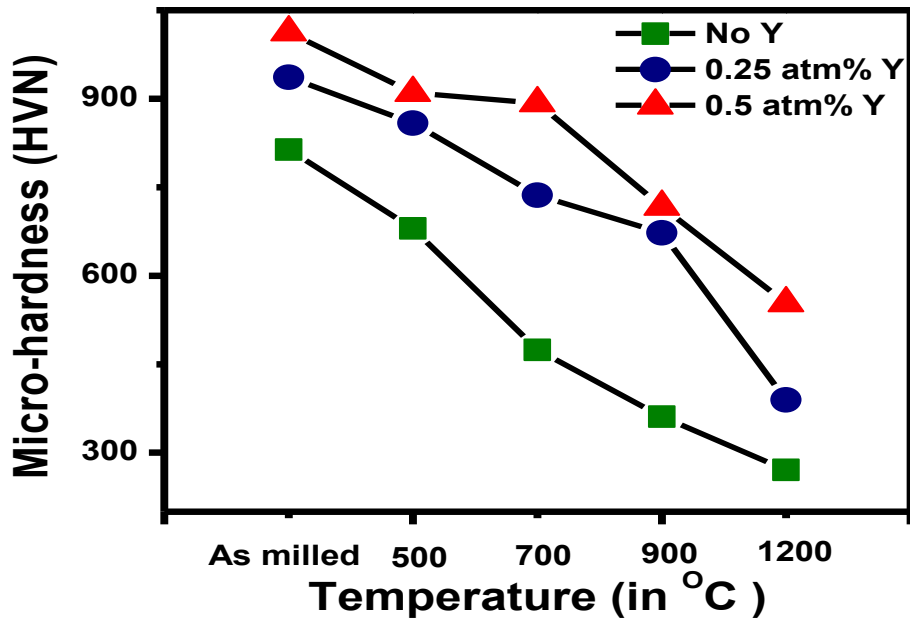


Figure 4.7: variation of crystallite size with different temperature of various compositions

In the above plot, we observe that the crystallite size initially increases with increase with anneal temperature in all 3 compositions. The crystallite size then decreases with temperature rise beyond 900°C. While in case of 0.25%Y, crystallite size increases progressively with temperature, a gradual increase upto 500°C followed by a near constant value upto 700°C and then a very sharp rise till 900°C is obtained in case of pure Fe. However in case of 0.5% Y, a drop in crystallite size occurs from 500°C to 700°C followed by a steep rise. The maximum crystallite sizes are observed at 900°C with the highest peak observed in case of pure Fe sample i.e 61.85 nm.



Figure

4.8: variation of Micro hardness with different temperature of various compositions

On an increase in anneal temperature a decrease in the micro hardness is observed. An exception is found at pure Fe where the hardness is found to decrease from 500°C to 700°C. The hardness is found to be higher for a higher % Y. Maximum micro hardness of 1012.8 VHN was obtained in the 0.5% Y sample in as milled condition while a minimum of 270.6 VHN was found in as milled condition annealed at 1200°C .

## 5. Conclusions :

- The hardness increases with increase in the amount of Y may be due to the mechanism of grain refinement strengthening and solid solution hardening. The hardness decreases with increase in annealing temperature. However, the rate of decrease in hardness with increase in annealing temperature is less with increase in amount of yttrium added.
- When considering different annealing temperatures, the crystallite size is found to decrease once the atom % Y exceeds 0.25 % , due to segregation of yttrium at the grain boundaries which pins the grain growth ,except for annealing at 700°C. On increasing the temperature of annealing, the crystallite size increases till 900 °C and then decreases. While considering different compositions, it is observed that the crystallite size obtained in samples having 0.5 % Y is significantly less than that of pure Fe and 0.25 atom% Y. The crystallite size of Fe-0.25 atom% Y is marginally below pure Fe till 500 °C but is considerably less when annealed at higher temperatures. This shows that the pinning effect of Y is more effective when atom % Y exceeds 0.25%.
- The lattice strain increases sharply with increase in yttrium content, when annealed at 500 °C and in as milled state. On further increasing of annealing temperature, it is found that the lattice strain increases upto yttrium content of 0.25 atom % and on further yttrium addition , the lattice strain decreases ; as in cases of annealing at 700 °C and 900°C. When annealed at 1200 °C , there is a decrease in lattice strain due to high temperature annealing which dominates the increase due to addition of yttrium. .

## **6.Scope for further work**

1. Further tests can be done by changing the parameters of mechanical milling like milling time, ball to powder weight ratio or addition of a process control agent and then optimizing the results.
2. There is further scope for improvement in mechanical properties if compaction can be done using advanced techniques like hot isostatic pressing.
3. Use of a different binder can bring forth different results.



## References :

1. K.A. Darling, B.K. VanLeeuwen, J.E. Semones, C.C. Koch, R.O. Scattergood, L.J. Kecskes, S.N. Mathaudhu, *Materials Science and Engineering A* 528 (2011) 4365–
2. Prashanth KG, Scudino S, Murty BS, Eckert J. Crystallization kinetics and consolidation of mechanically alloyed Al70Y16Ni10Co4 glassy powders, *Journal of Alloys and Compounds*, 477 (2009): pp. 171-177
3. Hasan Kotan, Kris A. Darling, Mostafa Saber, Carl C. Koch, Ronald O. Scattergood, *Journal of Alloys and Compounds* 551 (2013) 621–629
4. LIU Dong-hua, LIU Yong, ZHAO Da-peng, WANG Yan, FANG Jing-hua, WEN Yu-ren, LIU Zu-ming, *Transactions Nonferrous Met. Soc. China* 20(2010) 831-838
5. H. Kotan, M. Saber, C.C. Koch, R.O. Scattergood, *Materials Science and Engineering A* 552 (2012) 310– 315
6. D. Cui, J. Jiang, G. Cao, E. Xiao, X. Qu, *J. Univ. Sci. Technol. Beijing* 15 (2008) 150–154.
7. C. C. Koch, *Nanostructured Materials*. Vol. 9. pp. 13-22.1997
8. M.A. Meyers, A. Mishra, D.J. Benson, *Prog. Mater. Sci.* 51 (2006) 427–556.
9. Suryanarayana C. Mechanical alloying and Milling, *Progress in Materials Science* 46 (2001): pp. 1-184
10. C. C. Koch. (2002). *Nanostructured Materials - Processing, Properties, and Applications*. William Andrew Publishing.
11. K. Wolski, G. Le Caer, P. Delcroix, R. Fillit, F. Th6venot, J. Le Coze, *Materials ScienceandEngineeringA* 207 (1996) 97-104
12. F. Tehrani, M.H. Abbasi, M.A. Golozar, M. Panjepour, *Materials Science and Engineering A* 528 (2011) 3961–3966
13. F. Hadeifa, A. Otmania, A. Djekounb, J.M. Grenèche, *Materials characterization* 62 (2011)751 – 759
14. J.Z. Jiang, C. Gente, R. Bormann, *Materials Science and Engineering A*242 (1998) 268–277
15. T. R. Malow and C. C. Koch, *Acta mater.* Vol. 45, No. 5, pp. 2177-2186, 1997
16. Atkinson, H. V., *Acta metall.*, 1988, 36, 469-491
17. Bolling, G. F. and Winegard, W. C., *Acta metall.* 1958,6, 283-287.
18. Grey, E. A. and Higgins, G. T., *Actametall*, 1973, 21,309-321.
19. Andersen and O. Grong, *Actametall, mater.* Vol. 43, No. 7, pp. 2673-2688, 1995

20. H. Natter, M.-S. Löffler, C.E. Krill and R. Hempelmann, *Scripta mater.* 44 (2001) 2321–2325
21. J. M. Lifshitz and V. V. Slyozov, *J. Phys. Chem. Solids* 19, 35 (1961)
22. C. Wagner, *Z. Electrochem.* 65, 581 (1961)
23. J. C. Ion, K. E. Easterling and M. F. Ashby, *Acta metall.* 32, 1949 (1984).
24. K. Lu, Z.F. Dong, I. Bakonyi, A. Cziraki, *Acta Metall. Mater.* 45 (1997) 2177
25. K.A. Darling, B.K. VanLeeuwen, J.E. Semones, C.C. Koch, R.O. Scattergood, L.J. Kecskes, S.N. Mathaudhu, *Materials Science and Engineering A* 528 (2011) 4365–4371
26. Phase transformations in metals and alloys, D.A. Porter, & K.E. Easterling, Chapman & Hall, p140-142.
27. Kunok Chang, Long-Qing Chen, *Modelling and simulation in material science and engineering* 20 (2012) 055004 (11pp)
28. N. Moelans, B. Blanpain, P. Wollants, *ActaMaterialia* 55 (2007) 2173–2182
29. AzmirHarun, Elizabeth A. Holm, Mike P. Clode, Mark A. Miodownik, *ActaMaterialia* 54 (2006) 3261–3273
30. Zheng Chen, Feng Liu, Xiaoqin Yang, ChengjinShen, Yu Fan, *Journal of Alloys and Compounds* 509 (2011) 7109–7115
31. Kris A. Darling, Ryan N. Chan, Patrick Z. Wong, Jonathan E. Semones, Ronald O. Scattergood and Carl C. Koch, *ScriptaMaterialia* 59 (2008) 530–533
32. A. Molinari, S. Libardi, M. Leoni, P. Scardi, *ActaMaterialia* 58 (2010) 963–966
33. J. Svejcar, E. Dorazil, P. Pacl, P. Horky, *Journal of Magnetism and Magnetic Materials* 19 (1980) 45-48
34. Heather A. Murdoch, Christopher A. Schuh, *ActaMaterialia* 61 (2013) 2121–2132
35. G.M. Pharr, W.C. Oliver, *MRS Bulletin*, 7 (1992), p. 28
36. H.R. Wilde, A. Wehrstedt, *Materialprüfung*, 42 (2001), p. 468
37. C W Nieman, J R Weertman & R W Siegel, *scripta Met. et Muter.* 23(12),2013 (1989)
38. S K Ganapathi. and D A Rtgney, *Scripta Met. Er Mater.* 24,1675 (1990)
39. X Y Qin, X J Wu & L D Zhang, *Nanostructured Materials*, 5 (I), 101 (1995)
40. Yuchui Xiao & R James Kirkpatrick, *J. Muter. Res.* 10, 10 (1995)